

ECN's IBC solar cells in mass production environment: rise of a competitive back-contact module concept

Antonius R. Burgers, Ilkay Cesar, Nicolas Guillevin, Arthur W. Weeber and Jan M. Kroon, ECN Solar Energy, Petten, The Netherlands

Abstract

We present an n-type bifacial IBC solar cell that uses a simple process comparable to our industrially proven n-type cell process for conventional H-grid front- and rear-contacted n-PERT cells. The process is based on tube diffusion and a simultaneous single-step screen-print of the contacts to both polarities, and has been demonstrated on an industrial line at pilot scale. These IBC cells have been successfully integrated in foil-based modules, even using cells with thickness just below 100µm, enabling a route to significant reduction of silicon use. Further cost reductions with foils using cheaper aluminium instead of copper as conductor are described. The technology has huge potential to realize cost-effective PV electricity, for applications with both monofacial and bifacial illumination. Although the peak efficiency of 21.1% is currently modest, the process was embraced due to its inherent process simplicity.

The Mercury cell: enabler for low cost IBC

The Mercury Interdigitated Back Contact (IBC) cell [1] is a diffused screen printed IBC cell. The cell structure comprises an interdigitated boron-doped emitter and a phosphorous-doped back surface field (BSF) on the rear-side. A key feature is the boron-doped front floating emitter (FFE) on the front-side. The resulting Mercury IBC cell structure is shown in Figure 1 in comparison to an n-PERT cell. The analogy is clear, and the

opportunities to apply the same process as much as possible to both architectures will be discussed below.

The core of the IBC process is the same as in the n-PERT process, comprising single step BBr_3 and $POCl_3$ tube diffusions, identical SiN_x layers and screen printed fire-through metallisation. The tube diffusion processes used are designed to be suitable for industrial throughput, i.e. with lower cycle time and high load density. While the boron diffusion has been pivotal for the development of n-PERT, the competitiveness of an IBC cell with FFE is even more empowered by this process step. The FFE and the rear emitter are formed in the same, and single, diffusion step.

Structuring of the rear-side diffusion regions is based on conventional screen-printing processing. This patterning and diffusion approach greatly simplifies processing of the device and reduces manufacturing costs compared to complex and costly high resolution patterning techniques such as lithography or laser ablation processes. In addition, this approach offers a great flexibility in implementing different diffusion pattern designs and matching metallization and interconnection designs. Front-side and rear-side surface passivation and anti-reflecting coatings can be realized with industrial ALD (Atomic Layer Deposition) and PECVD (Plasma Enhanced Chemical Vapour Deposition) equipment respectively. The metallization consists of a firing-through Ag paste deposited in a single step, for both emitter and BSF, by screen-printing, and features an open grid design suitable for thin wafers and bifacial applications.

The case for n-type cells

p-type Al-BSF and PERC

The PV market is presently dominated by cells and modules with p-type multi- and monocrystalline front-to-back contacted solar cells [2], as we can see in Figure 2. The trusted p-type Al BSF cells are to date still the workhorse of the PV industry, explained in a large part by

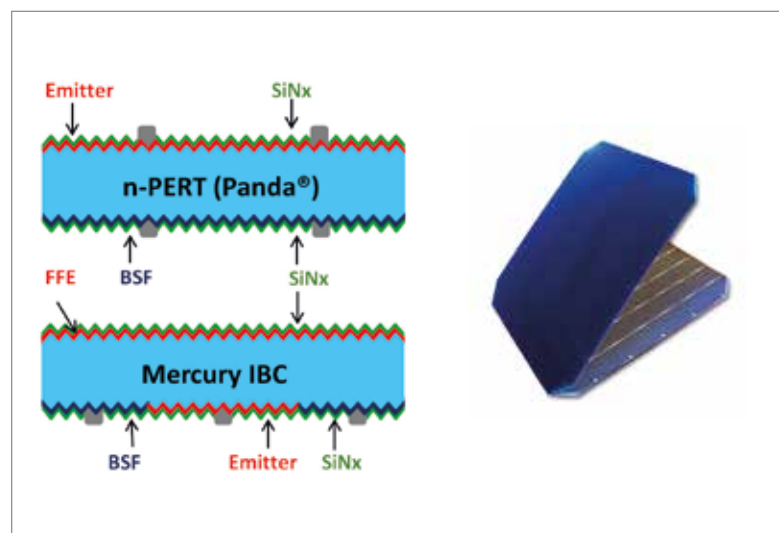


Figure 1. a) cross section of an FFE IBC cell; b) picture of front and rear side of an IBC cell.

the low cost and the simplicity of the process. Over recent years p-type Passivated Emitter and Rear Cell (PERC) cells have been successfully making a dent in the Al BSF cell dominance. The key innovation in the PERC cell over the Al-BSF cell is improving the passivation and light trapping of the rear side by means of a dielectric, making openings with laser processing in that dielectric, and then realizing local Al contacts. Although the PERC cell shares major process characteristics with the Al BSF steps, it does add to the complexity and cost of the process.

The Al-BSF cell and its modules are monofacial, because of the full aluminium metallization at the rear side. The basic PERC process also uses a full aluminium rear metallization as source for the local rear contacts, and hence is not bifacial. The PERC+ cell [3] addresses this by applying a partial aluminium metallization. Because of the lower conductivity of an open Al metallization, the integration of the cell with the interconnection and module technology becomes very important, in particular when aiming for bifacial modules.

Towards n-type cells

Solar cells based on n-type materials are generally considered and expected (See Figure 3) to enable significantly higher conversion efficiencies, and hence open a route to modules with lower cost of ownership. The potential for high efficiency is well documented and demonstrated, e.g. by Sunpower [4] and Panasonic [5].

The high conversion efficiency potential makes the n-type-based cells most attractive for back-contact concepts requiring high-quality material, such as IBC cells. In high-efficiency cells the collection efficiency for charge carriers is high, independent of whether they are generated at the front or rear side of the cell, thus enabling excellent bifaciality of the cells. High-efficiency n-type modules have the benefits of a better temperature coefficient, and converting a larger fraction of the incoming light to electricity instead of heat, leading to better kWh/kWp energy yield [6, 7]. Additionally, the higher module output power of the same size module reduces also the area-related costs of a PV system.

A bifacial module will, in addition to light impinging on the front side, also convert light that enters through the back side of the module into power. This brings about a gain of 10-30% [8] in power compared to a monofacial module. There is a large range in these bifacial gains, because they depend on a multitude of factors, such as the albedo of the surroundings, the elevation of the modules over the ground plane, the separation between modules, to mention just a few. Exploiting the bifaciality effectively increases the cell efficiency at little cost, reducing the area related system cost.

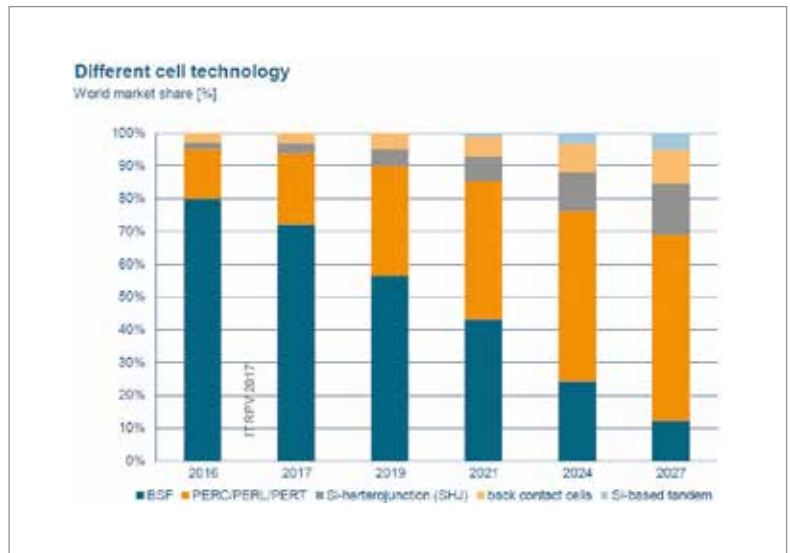


Figure 2. The actual and projected market shares of different cell types, ITRPV 2017.

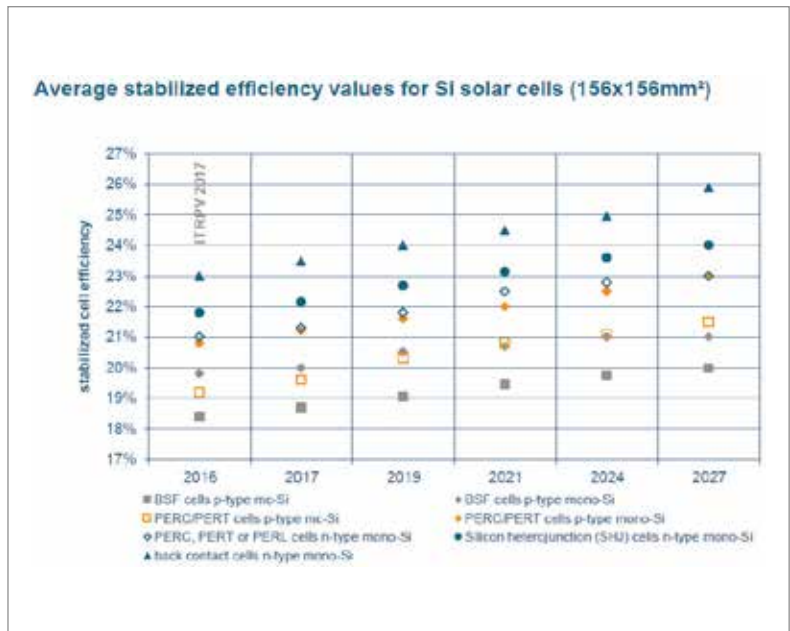


Figure 3. Projected development of the efficiency of different cell types, ITRPV 2017.

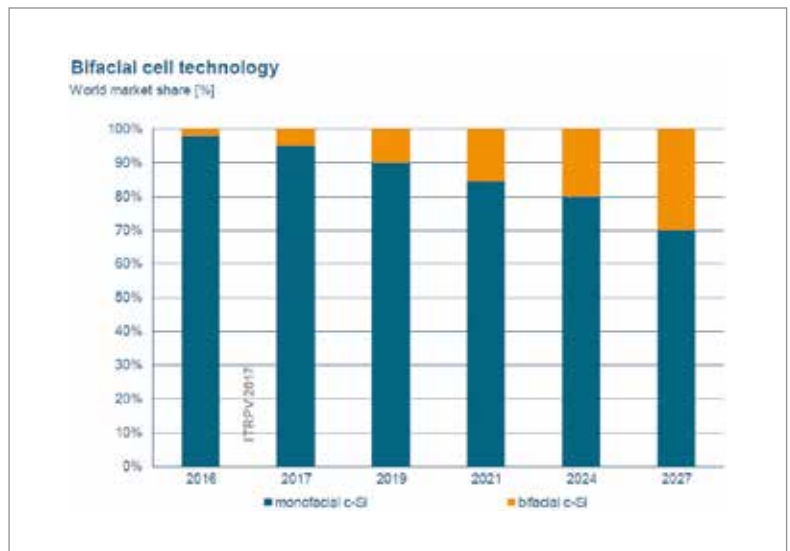


Figure 4. Actual and projected market share for mono- and bifacial modules, ITRPV 2017

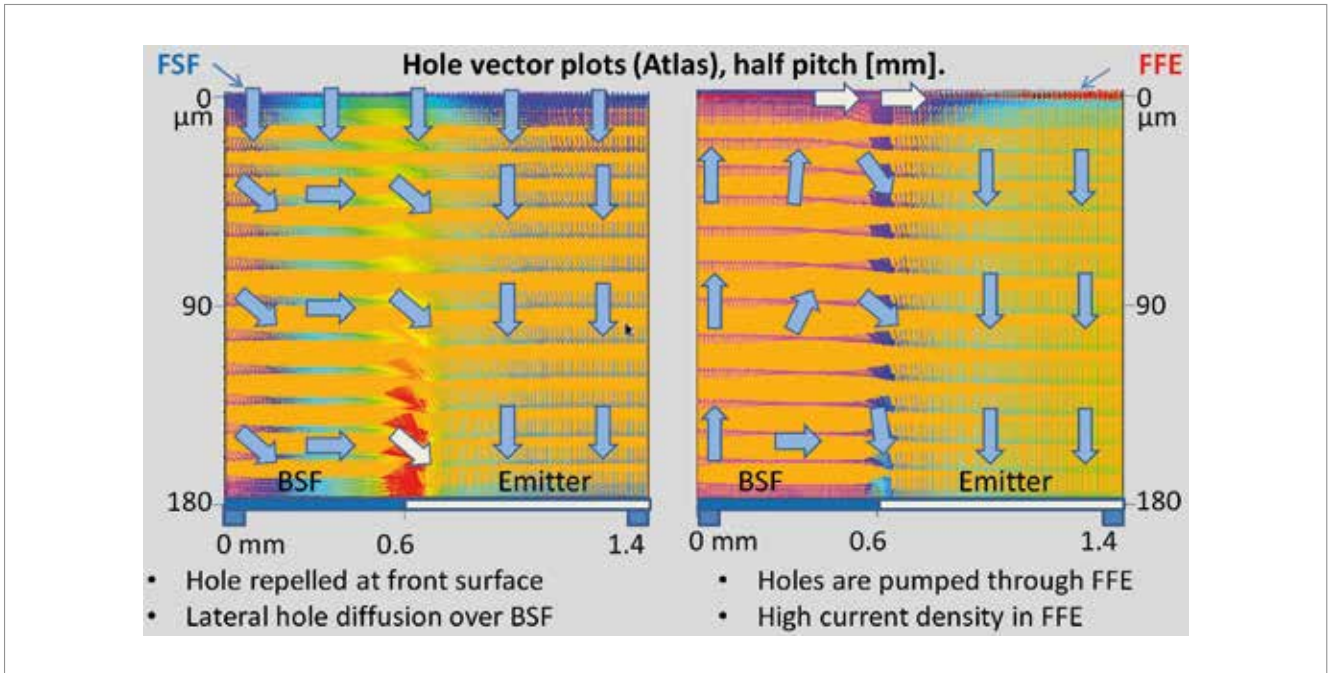


Figure 5. Comparison of hole current flow in a) FSF and b) FFE IBC structures

Front floating emitter for low cost IBC

Traditionally, IBC cells use a front surface field (FSF). If not properly designed, an FSF IBC cell can suffer from high recombination losses over the rear BSF, an effect referred to as “electrical

shading”. To mitigate the effect of electrical shading two approaches are available:

1. High-resolution processing: in an FSF cell the primary approach is to reduce lateral transport distances, in particular by realizing narrow

R | E | N | A | .

Speeding up your PERC line

Higher throughput at low cost for your production

Visit us at
SNEC PV
POWER EXPO
Booth
E3-355



RENA BatchTex N400
and monoTEX® process
Tunable pyramid size

Now
up to
8000
wph



RENA InOxSide+
Junction isolation and
adjustable rear side etch

Now
up to
5500
wph

More at
www.rena.com



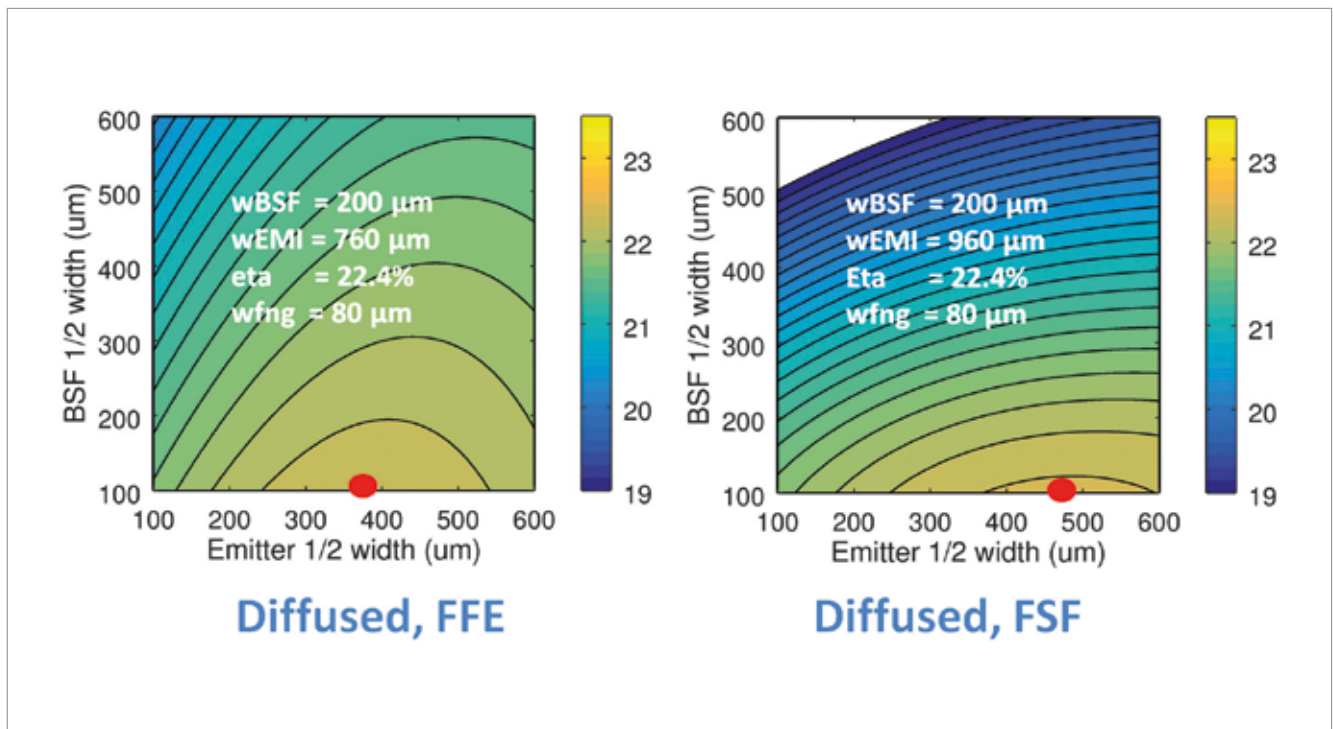


Figure 6. Cell efficiency as a function of emitter and BSF width for a) with an FFE and b) with an FSF. The white text gives the device parameters at the spot of the optimum (indicated by a red dot).

BSFs. This can be achieved by high-resolution patterning steps, which in general comes at a cost.

- Using a front floating emitter (FFE) we mitigate electrical shading with the FFE. This enables low-resolution processing, and hence opens up a route to lower cost processing.

Electrical shading and these two approaches will be explained in more detail in the next section.

Mitigating electrical shading with an FFE

In FSF IBC cells the p-n junctions are present only on the rear side of the cells. Hence minority carriers generated above the rear BSF need to diffuse laterally towards the nearest p-n junction (Figure 5a). Lateral transport distances are governed by the pitch in the rear cell geometry. If the distance towards the nearest p-n junction is relatively large, that increases the risk of recombination of the carriers on their way. Secondly, in order to drive the diffusion, a concentration gradient is required, with a high concentration of minorities above the BSF. This increases the injection level, and increases chances of recombination.

In an IBC cell with an FFE, a p-n junction is also formed at the front side, which is never more than a wafer thickness away for any carrier. Once collected in the FFE (see Figure 5b) carriers can travel laterally as majorities, without recombination losses. Over the rear emitter the majorities are re-injected into the base as minorities, and once again only need to cross the thickness of the wafer. This process of collection over the BSF and subsequent re-injection back

into the base over the rear p-n junction results in a “pumping effect”: transport of minority carriers from regions above the BSF to the rear emitter through the FFE with very little recombination losses.

To illustrate this, Figure 6 shows contour plots of the efficiency as a function of the unit cell design. The cell efficiency in IBC cells depends much more strongly on unit cell design than in conventional front rear contacted cells, such as the Al BSF cell and n-PERT cells, due to the importance of lateral transport of minority carriers in the base. Device simulations were done for multiple BSF-emitter width combinations, using J_0 values for a diffused IBC with firing through metallization, and the results were used to derive the contour plots. What we observe is that for FFE cells the efficiency holds up much better than for FSF cells as we move up along the y-axis and the BSF width is increased. For instance for the case of both BSF and emitter having a width of 1mm we observe an efficiency of well >21% for the FFE case, where the FSF case is already <20%.

Even with the FFE there are of course limits on the lateral transport distance, because of resistive losses in the FFE. However an FFE radically expands the design space of IBC cells, thereby offering ways to reduce process complexity and thus cost. In addition, being able to increase the pitch size on the rear side reduces the metal coverage on the rear side, and in turn enhances the bifaciality of the IBC cell. If p-n junctions would have an adverse effect, an FFE allows their impact to be reduced, by reducing the number of p-n

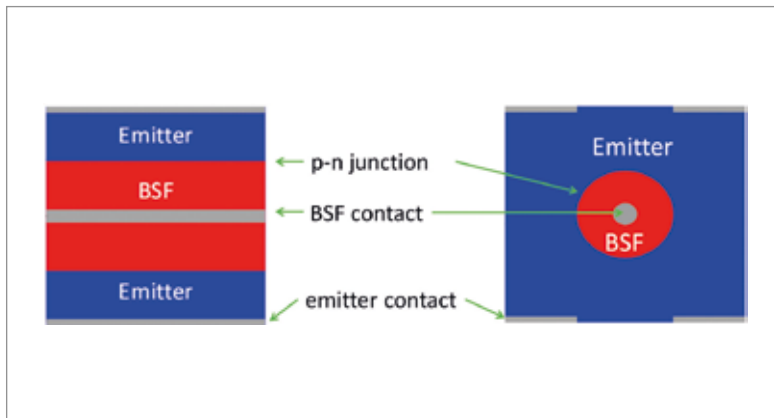


Figure 7. Changing from linear diffusion to island geometry.

Processing step	Mercury IBC	n-PERT
diffusions	boron/phosphorous	
diffusion patterning	screen-printed patterning	no
edge isolation	no	yes
surface passivation	wet chemical and dielectrics	
metallization	all-in-one paste single print	1. Ag/Al front print 2. Ag rear print

Table 1. Comparing major process steps in n-PERT and Mercury IBC.

junctions.

Synergy and simplicity in process flows

The continuing success of the Al-BSF cells makes one wonder what can be learnt from this process, and how these lessons can be applied to new technologies. A key factor is the very simplicity of the process. At the core of the process, one diffuses a phosphorous emitter into the future light receiving front side, deposits a hydrogen rich silicon nitride (SiN_xH) film at the front, prints the rear side fully with aluminium paste, and applies an H-grid pattern with Ag paste on the front side.

Then during the firing step near magic occurs. The Ag paste fires through the SiN_xH film and makes an ohmic contact to the emitter. The temperature occurring during the firing makes the hydrogen in the SiN_xH film mobile, and allows the hydrogen to improve both bulk and surface passivation. At the same time the aluminium dissolves some of the silicon, leaving a BSF passivating the rear side on cooling down and forming an ohmic contact to the rear.

The Mercury IBC cell was conceived with this success in mind, the boron diffusion serving similarly as an important multifunction process step:

1. The developed diffusion process results in passivation of the emitter – BSF junctions at the rear side, as well as a perfectly passivated wafer edge. Both process features circumvent a laborious and expensive gap and edge isolation process [9].
2. It is a one step process preparing the front and

rear emitters for surface passivation and rear contact formation.

3. The entire surface with all its diffused layers, including the rear BSF-emitter junctions, can be passivated using regular wet chemistry steps and dielectric layers. Because of the presence of diffused layers, inversion layers have less impact on the surface passivating quality, and a wide range of passivation options is available and suitable for passivation of polarities at the same time.
4. A conductive FFE is realized that enables large patterning feature sizes for ease of manufacturing and more freedom in module integration, which will be discussed in the module section of this paper. The large feature size in turn enables high bifaciality, and renders the cell less prone to hi-hi p-n junction issues.

The patterning of the rear-side diffusions is an extra step, but this is offset in other steps, as shown in Table 1. The presence of all contacts on the rear side allows for all-in-one print of the metallization, ready for soldering.

Demonstration in a pilot line setting

Because the process is close to existing n-PERT processing, and the requirements on resolution for the FFE IBC cells are lower, the cell concept maps well to industry-scale screen-printed processing. Similar process equipment as well as process parameters are used without increasing the number of major manufacturing steps, making the Mercury process compatible with an industrial-scale production and throughput. Pilot processing in an industrial environment therefore offers a great opportunity for the Mercury IBC technology to gain in maturity by rapidly acquiring knowledge on manufacturability. Yingli has successfully implemented this process [10, 11]. First working cells were achieved within three months of the start of the project.

Cell efficiency results

In Table 2 the I-V parameters of our best IBC cell are shown. The bifaciality factor reaching 83% here is excellent, considering this is an IBC cell. In an IBC cell all metallization is on one side of the cell, the rear side, limiting the bifaciality. If for example the metallization coverage on the rear side is say 12%, the bifaciality factor cannot exceed 88%. On encapsulation the bifaciality can increase, by virtue of trapping of the light reflected diffusely off the metallization at the glass-air interface.

Note that ISC Konstanz has developed a similar concept, the Zebra cell (12). For the Zebra cell efficiencies up to 21.9% [13] have been reported.

Performance limitations in current cells

By measuring the recombination losses at surfaces and interface we determined that the efficiency

of our IBC cell is to a large extent limited by recombination at the screen printed contacts, in particular the emitter contact, and at the passivating quality of the BSF, as can be observed from Table 3.

We have seen that for pastes for phosphorous emitters and boron emitters huge improvements have been realized over the years, realizing better J_o and r_c values on these emitters with increasing resistivity. Current development of the Mercury design has been limited by the performance of the all-in-one paste. We think there is ample room for improvement in the short term for all-in-one pastes that contact both phosphorous and boron diffusions. Since developing novel pastes needs more effort, we investigate alternative routes like so called BSF islands.

BSF island: Mercury IBC cells with localized BSF diffusion

The recombination activity in the cell is dominated by the emitter contacts and the heavily doped BSF area. Therefore, reducing both the BSF area and the emitter contact fraction is a route to decrease the recombination in the cell and therefore enhance the cell performance.

Depending on the contact width and the screen printing tolerances, a minimum width of the passivated BSF area is required, which is typically more than 300 μm . In a one-dimensional interdigitated finger design (Figure 7a) the only option to reduce the BSF area fraction further is then to increase the emitter width, but this induces large transport losses. Therefore, we reduced the BSF length within the unit cell [14], and in this way we created “islands” of BSF surrounded by the rear-side emitter, as shown in Figure 7. The BSF area reduction will mainly improve the passivation of the cell, and increase the voltage, and increase current by avoiding recombination. In the Mercury IBC cell case, electrical shading is not a major issue due to the collecting and transporting front floating emitter, hence reducing the BSF area is not required from a standpoint of electrical shading.

In Table 5 the breakdown in J_o contributions between the two different geometries is compared. In particular the contribution of the emitter contact to the recombination has reduced.

In the longer term, passivated contacts open a route to higher efficiencies. For n-PERT the so called PERPoly cell has been developed. In the PERPoly cell the rear phosphorous BSF is replaced

with an industrial rear poly silicon BSF [15, 16], that achieves markedly lower J_o values for the contacts while still using firing through contacts, (See Table 6) and has resulted already in a 0.5% absolute efficiency gain for PERPoly cells compared to n-PERT references.

Because the IBC Mercury process is very close to the n-PERT process, improved contacts for n-PERT can be transferred to n-IBC with relative ease.

IBC cell-based modules

Flexibility of the diffusion pattern and metallization grid designs offers freedom when it comes to the choice of module interconnection technology. Based on the current metallization grid design, which includes interconnection pads, the cells can be readily processed into modules using ECN’s foil-based interconnection technology [17, 18]. ECN’s module manufacturing technology is based on an interconnection foil with integrated conductor layer (e.g. copper or aluminium), on which the cells are electrically contacted using an electrically conductive adhesive (ECA). Compared to a tabbed interconnection technology, the interconnection foil allows reduction of the module series resistance by using more interconnect metal (more cross-sectional area) and thereby reduces the cell-to-module FF loss [19]. Also, the module manufacturing based on integrated back-foil can be done with higher yield and reduced interconnection-process-related stress, allowing use of (much) thinner cells and therefore offering additional cost reduction possibilities. This type of module has passed full IEC testing [20].

Full size 60 cell – thin wafer – IBC cell module

To prove that we are ready for the future silicon wafer thickness, we have processed modules with cells nearly half as thick as today’s standard. These fragile wafers are incompatible with current standard tabber-stringer processes, because the process yield is low.

A batch of 156 thin wafers (starting thickness 120um, final thickness 95um) has been processed to Mercury IBC cells at ECN. The best 60 cells of this

Area	J_{sc} (mA/cm ²)	V_{oc} (mV)	FF (%)	Eta (%)	Bifaciality factor
239	41.2	653	78.4	21.1	83%

Table 2. I-V parameters of the best Mercury IBC cell measured at ECN. Short circuit current is corrected for spectral mismatch.

bulk	J_o corrected for area fraction (mA/cm ²)			BSF	total	V_{oc} @300K (mV)
	FFE	emitter				
J_o	J_o	J_o	$J_{o,contact}$	J_o	$J_{o,contact}^t$	J_{ototal}
11	40	22	149	89	45	357
						658

Table 3. Area weighted J_o breakdown for IBC cell.

batch have been integrated

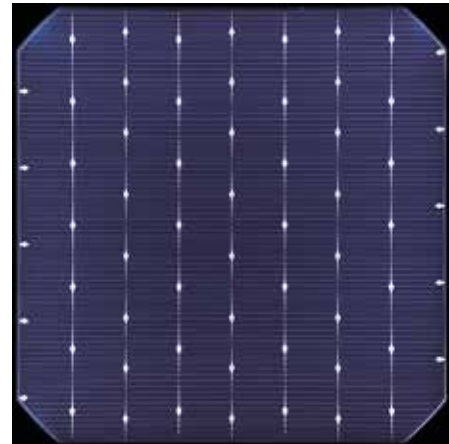
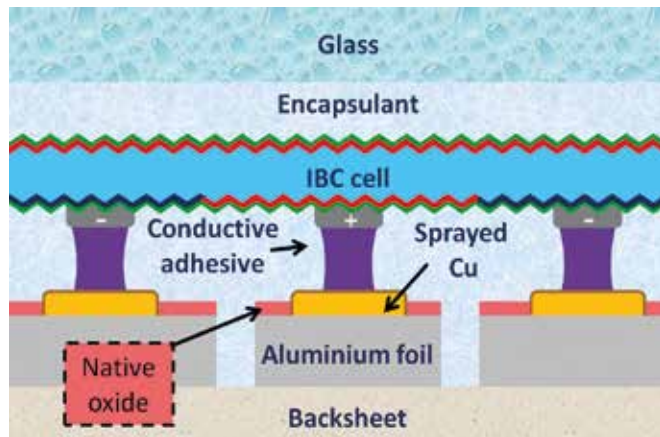


Figure 8. a) Interconnection by means of the Cu cold spray method (schematic); b) 62-pad cell interconnect pattern.

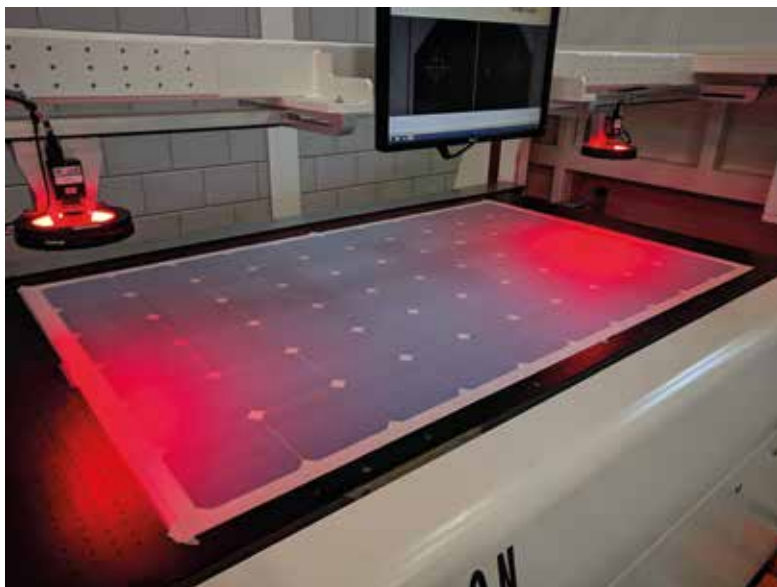


Figure 9: the pick and place stage for the cells on the foil. Picture taken at Eurolab BV, NL.

	J_{sc} [mA/cm ²]	V_{oc} [V]	FF [%]	Efficiency [%]
Reference	38.9	0.653	79.1	20.1
BSF islands	39.9	0.663	77.9	20.6

Table 4. I-V results for the BSF island geometry.

case	bulk	J_0 corrected for area fraction (mA/cm ²)				BSF	total	V_{oc} @300K (mV)
		FFE	emitter					
	J_0	J_0	J_0	$J_{0,contact}$	J_0	$J_{0,contact}$	J_{total}	
linear	11	40	22	149	89	45	357	658
BSF island	11	40	30	60	60	19	220	670

Table 5. J_0 breakdown for IBC cell.

polySi thick (nm)	n-poly j_0 (fA/cm ²)	n-poly/Ag paste $j_{0,c}$ (fA/cm ²)	p-poly j_0 (fA/cm ²)	p-poly/AgAl paste $j_{0,c}$ (fA/cm ²)
100	1.3	1084 (461)	5.6	796 (103)
200	2.7	386 (22)	5.7	319 (40)

Table 6. J_0 values for n-type and p-type polysilicon layers with firing-through contacts.

in a foil-based module using copper as the conductor layer, without any breakage. The one-sun power output of this module was measured at 277W, while the summed power of the individual cells was 278W. Hence the cell-to-module loss was <1%. This is a good number, considering that:

- The foil-based approach allows close packing of the cells, with little spacing between the cells. The white space in a conventional tabbed module actually contributes significantly to the module current.
- In a front metallized cell, after encapsulation, light reflected diffusely off the metallization is trapped in the front glass and encapsulant and can re-impinge on the non-metallized cell, contributing to the current of the cell, and hereby effectively reducing the metal grid shading. This effect is absent in IBC cells.

Noting that the silicon wafer comprises about 40% of the cost of the module in 2017 [2], being able to integrate thin cells with high yield in a module opens a route to saving on wafer cost. A paper describing this module and module technology in more detail, and its cost benefits will be presented at the WCPEC-7 [21].

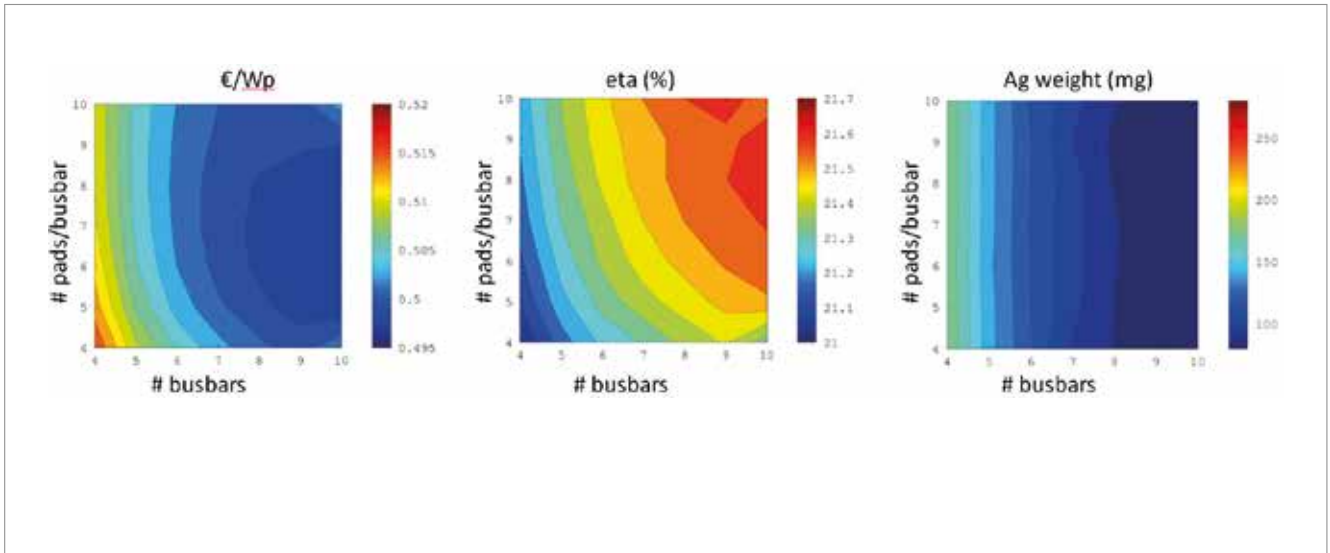


Figure 10: Interconnect design and Ag consumption a) €/Wp; b) efficiency; c) Ag used per cell based on cost levels in 2016.

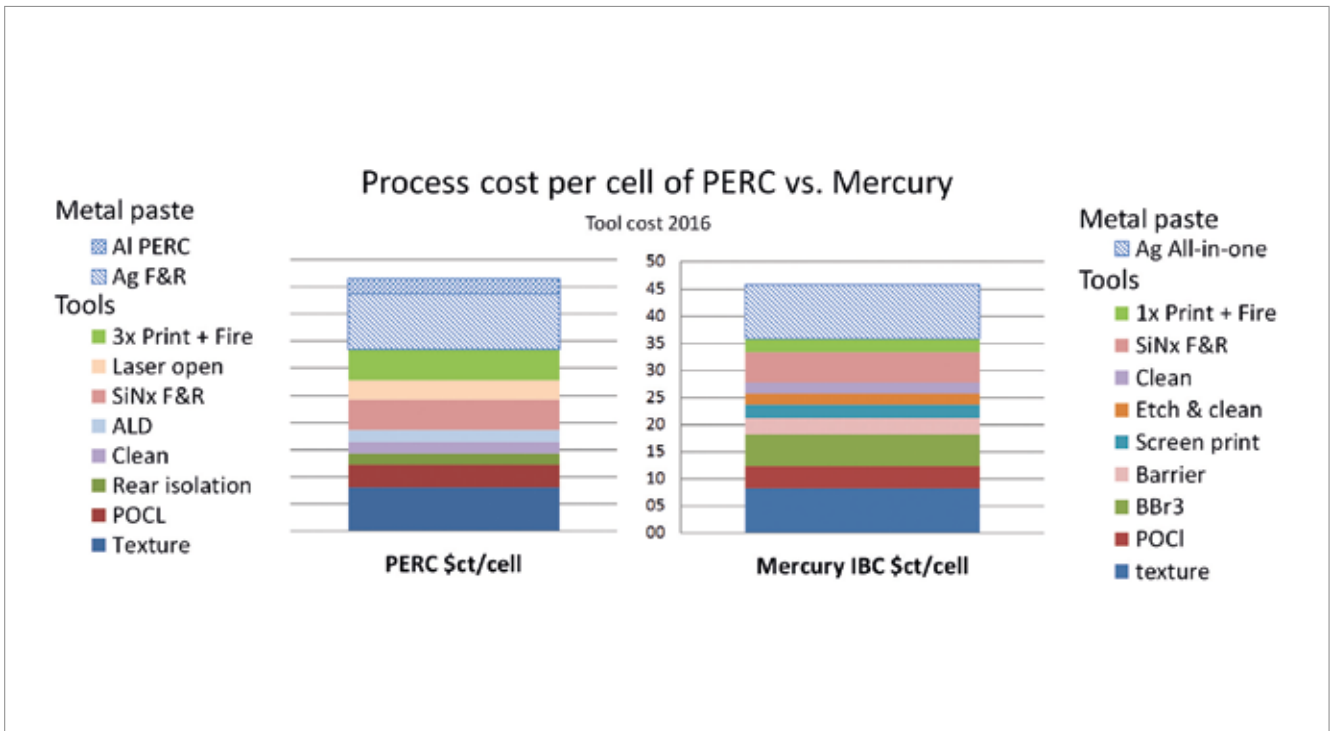


Figure 11. Cost breakdown of the cell processing cost for PERC and Mercury.

Aluminium based rear foils

Replacing the Cu conductor layer with Al can result in a cost saving of about 2% on module level. However it is much more difficult to make an electrical contact with ECA to Al than to Cu, because of the native oxide that is present on Al. The copper cold-spray method [22, 23] is a method to deposit copper particles on aluminium conductive foil, while opening the oxide, and allows to establish a both mechanically and electrically good and stable localized contact between the solar cells and the aluminium, as illustrated in Figure 8a.

Figure 8a is a schematic in the sense that connections are not made directly to the individual fingers. Instead in Figure 8b we show that the cell has an interdigitated finger pattern, with busbars of alternating polarity. On the busbars there are in this case 62 pads (~30 per polarity) provided for application of ECA. The corresponding positions on the rear foil are the locations where Cu needs to be present.

Several IBC four-cell mini-modules using cold-sprayed aluminium as the conductive back foil were fabricated and passed selected IEC 61215 tests (damp heat at 85°C/85% RH and thermal

cycling between -40 and 85 °C), demonstrating the large potential of this cost reduction approach. An upcoming paper describing this method and the benefits of the back contact module technology will be presented in more detail at the WCPEC-7 [21].

Foil design and cell Ag cost

The foil-based approach is an enabler to reduce Ag cost, by moving conduction from Ag on the cell to the metal on the rear foil. By increasing the number of interconnects, the average distance of any point on the cell to nearest interconnect decreases, reducing the requirements on Ag conductivity.

The requirement on Ag consumption is illustrated in Figure 10. For each combination of the number of busbars and the number of pads/busbar, the unit cell design (BSF width, emitter width) was picked that gives the best €/Wp. The amount of ECA required per interconnect was assumed to be fixed. The best cell efficiencies are reached in the upper right corner, for a high number of busbars (short fingers) and a high number of interconnects (short busbars). For lower numbers of busbars, the fingers become long, and much Ag is required to maintain a sufficient FF. For high numbers of pads/busbar the ECA cost comes into play, leading to an optimum in this case of around nine busbars and seven interconnects per busbar. The Ag consumption at that point is in the order of 100mg. [10] reports our evolution in cell and processing from a design with ~30 contact pads to ~81 pads currently, allowing us to reduce the Ag consumption.

Cost comparison Mercury IBC with PERC

In Figure 11 a breakdown is shown of the processing cost for PERC and Mercury per wafer. The boron diffusion is a relatively expensive step; however in the Mercury process we prevent other costly steps, such as laser opening and multiple print steps, ending up with comparable cost.

Conclusions

Mercury cells open up a route to manufacturable n-type IBC cells, building upon existing n-PERT technology, enabling high efficiency and good bifaciality. The cells feature a simple process, a well passivated gapless rear p-n junction, without need for edge isolation. The progress is currently limited by the performance of the silver paste. For monofacial application the combination with foil-based modules with aluminium as the main conductor allows significant cost reductions. We demonstrated Technology Readiness Level 6 processing of ultra-thin silicon wafers in to IBC modules without yield loss. We look forward to advancing these concepts with our partners.

Acknowledgements

We are grateful for the financial support from the Dutch government through the Topsector Energy Subsidies of the Ministry of Economic Affairs of the Netherlands and the European Commission via the funded project Cheetah (GA nr. 609788).

References

- [1] Cesar, I. et al. 2104, "Mercury: A Back Junction Back Contact Front Floating Emitter Cell with Novel Design for High Efficiency and Simplified Processing", *Energy Procedia*, Volume 55, 633-642.
- [2] International Technology Roadmap for Photovoltaic (ITRPV), Eighth Edition 2017.
- [3] Dullweber T. et al, 2018, "Industrial implementation of bifacial PERC+ solar cells and modules", *PV international*, Edition 38, page 46.
- [4] Smith, D. et al. 2014, "Towards the Practical Limits of Silicon Solar Cells", *Proc. 40th IEEE PVSC*.
- [5] "Panasonic HIT solar cell achieves world's highest energy conversion efficiency of 25.6% at research level", Public Relations Development Office, Panasonic Corp., Osaka, Japan, April 2014.
- [6] Smith, D. et al. 2012, "Generation III high efficiency lower cost technology: Transition to full scale manufacturing", 38th IEEE Photovoltaic Specialists Conference, Austin, TX, 001594-001597.
- [7] "Panasonic HIT Solar Module Achieved World's Highest Output Temperature Coefficient at -0.258%/°C", Public Relations Development Office, Panasonic Corp., Osaka, Japan, May 2017.
- [8] Janssen, G., Van Aken, B., Carr, A., Mewe. 2015, "Outdoor performance of bifacial modules by measurements and modelling", *Energy Procedia* 77, 364-373.
- [9] Spinelli, P. et al. 2017, "Quantification of p-n junction Recombination in Interdigitated Back-Contact Crystalline Silicon Solar Cells", *IEEE Journal of Photovoltaics*, Vol 7, 1176.
- [10] Guillevin, N. et al. 2017, "Pilot line results of n-type IBC cell process in mass production environment", 33rd EU-PVSEC, Amsterdam.
- [11] Liu, D. et al. 2018, "Development of Large-Area Bifacial Interdigitated-Back-Contact (IBC) Solar cell with Industrial Production Environment", submitted to WCPEC-7: 45th IEEE PVSC, 28th PVSEC, 34th EU PVSEC, Hawaii.
- [12] Mihailetchi, V., Chu, H., Galbiati, G. 2015, "A comparison study of n-type PERT and IBC cell concepts with screen printed contacts", *Energy Procedia* 77, 534 – 539.
- [13] Galbiati, G. et al. 2106, "Large area IBC Zebra solar cells in pilot production: the results of FP7 Hercules project", 32nd EU-PVSEC.
- [14] Mewe, A. et al. 2017, "BSF islands for reduced recombination in IBC cells", *IEEE PVSEC-44*, Washington DC.
- [15] Stodolny, M. et al. 2016, "n-Type Polysilicon Passivating Contacts for Industrial Bifacial n-PERT

Cells”, EU-PVSEC, 2016.

[16] Çiftpinar, H., Stodolny, M., Wu, Y., Janssen, G., Löffler, J., Schmitz, J., Lenes, M., Luchies, J.-M., Geerligs, L. 2017, “Study of screen printed metallization for polysilicon based passivating contacts”, *Energy Procedia*, Volume 124, 851-861.

[17] Bennett, I.J., Eerenstein, W., Rosca, V. 2013, “Reducing the cost of back-contact module technology”, *Energy Procedia* 2013; 38:329-33.

[18] Bende, E.E., Van Aken, B.B. 2015, “The effect of reduced silver paste consumption on the cost per Wp for tab-based modules and conductive-foil based modules”, *Energy Procedia* 2015; 67:163-74.

[19] Van Aken, B., Slooff-Hoek, L. 2016, “Positive cell-to-module change: Getting more power out of back-contact modules”, *Photovoltaics International*, Vol. 33, 97-105.

[20] Eerenstein, W. et al., 2010, “Climate chamber test results of MWT back contact modules”, 25th European Photovoltaic Solar Energy Conference and Exhibition/5th World Conference on Photovoltaic Energy Conversion, Valencia, Spain.

[21] Newman, B., Kroon, J., Guillevin, N., Okel L., Sommeling, P., Goris, M., Eerenstein, W., Gonzalez, J. 2018, “Materials Development and Increased Module Efficiency for 15% Cost Reduction of Reduction of Back Contact Modules”. Submitted to WCPEC-7: 45th IEEE PVSC, 28th PVSEC, 34th EU PVSEC, Hawaii, 2018.

[22] Goris, M., Bennett, I., Eerenstein, W. 2014, “Aluminium Foil and Cold Spray Copper Technology as Cost Reduction Process Step in Back-contact Module Design”, *Energy Procedia* Volume 55, 342-347.

[23] Goris, M.J.A.A., Kikkert, B.W.J., Kroon, J.M., Rozema, K., Bennett, I.J., Verlaak, J. 2016, “Production of low cost back contact based PV modules”, 32nd European Photovoltaic Solar Energy Conference, Munich, Germany, p. 99-104.

.....

About the Authors



Antonius (Teun) Burgers received a degree in mathematics from Leiden University in 1984 and a doctorate in natural sciences from the University of Utrecht in 2005. He joined ECN in 1985. Since 1992 he has been working in the field of solar energy, both in experimental physics and modelling of solar cell physics. From 2010 to 2012 he has been involved in n-PERT development and its industrial transfer. Currently he is focusing on bifacial IBC solar cell technology and bifacial applications in general.



Ilkay Cesar received a master’s degree in chemical engineering from the TU Delft, in the Netherlands and a Ph.D. in chemistry and chemical engineering from the EPFL in Switzerland. He received the “Du

Pont Material award” for excellent research in the field of material science related to solar fuels for his Ph.D. dissertation. He joined ECN in 2007 and is currently focusing on the industrialization of new silicon PV technology. The recent implementation of bifacial IBC solar cell technology at Yingli Solar is a good example of this work.



Nicolas Guillevin studied at the National Engineering School of Industrial Ceramics in Limoges (France) where he obtained in 2007 a master’s degree in the field of material science and process engineering. In 2008, he joined the device architecture and integration group at ECN Solar in the Netherlands where he started his research activities on the development of n-type silicon solar cells. He currently focuses his work on the design and optimization of back-contact solar cell and module technologies.



Jan Kroon studied chemistry at the University of Amsterdam and received his Ph.D. in the field of Physical Organic Chemistry in 1992. He worked as postdoctoral fellow on organic solar cells at the Wageningen University. He joined ECN Solar Energy in 1996 where he worked as project and programme manager of organic-based PV technologies until June 2013. Since then, he has been active as senior project manager in the ECN PV module technology group and currently programme coordinator back-contact crystalline Si cells and modules. He is an experienced coordinator and manager of several national and international (European) projects.



Arthur Weeber studied physics and chemical engineering at the University of Amsterdam (UvA). After having received his Ph.D. at the same university in 1988, he joined ECN. Since 1992 he has been working in the field of photovoltaics and has coordinated large national and international projects. In 2015, Arthur was appointed as full professor in the PhotoVoltaic Materials and Devices group at Delft University of Technology. Since then he has been combining this professorship with his work at ECN Solar Energy.

.....

Enquiries

ECN Solar Energy
 PO Box 1, NL-1755 ZG Petten, The Netherlands
 +31885154761
 E-mail: burgers@ecn.nl (Teun Burgers)
 E-mail: cesar@ecn.nl (Kay Cesar)
 E-mail: vanstrien@ecn.nl (Wouter van Strien)